Title
Aldehyde dehydrogenase 1a1 mediates a GABA synthesis pathway in midbrain dopaminergic neurons

Journal
Science, 350(6256)

ISSN
0036-8075

Authors
Kim, Jae-Ick
Ganesan, Subhashree
Luo, Sarah X
et al.

Publication Date
2015-10-02

DOI
10.1126/science.aac4690

Peer reviewed

NEUROTRANSMISSION

Aldehyde dehydrogenase 1a1 mediates a GABA synthesis pathway in midbrain dopaminergic neurons

Jae-Ick Kim,[1] Subhashree Ganesan,[1] Sarah X. Luo,[2,3] Yu-Wei Wu,[1] Esther Park,[1] Eric J. Huang,[2,3,4] Lu Chen,[1] Jun B. Ding[1,5]*

Midbrain dopamine neurons are an essential component of the basal ganglia circuitry, playing key roles in the control of fine movement and reward. Recently, it has been demonstrated that γ-aminobutyric acid (GABA), the chief inhibitory neurotransmitter, is co-released by dopamine neurons. Here, we show that GABA co-release in dopamine neurons does not use the conventional GABA-synthesizing enzymes, glutamate decarboxylases GAD65 and GAD67. Our experiments reveal an evolutionarily conserved GABA synthesis pathway mediated by aldehyde dehydrogenase 1a1 (ALDH1a1). Moreover, GABA co-release is modulated by ethanol (EtOH) at concentrations seen in blood alcohol after binge drinking, and diminished ALDH1a1 leads to enhanced alcohol consumption and preference. These findings provide insights into the functional role of GABA co-release in midbrain dopamine neurons, which may be essential for reward-based behavior and addiction.

Midbrain dopamine (DA) neurons are important for fine-movement control, motivation, and reward-based learning (*1*, *2*). Dysfunction of dopaminergic systems leads to movement disorders, such as Parkinson's disease, and various forms of addiction and drug abuse (*3*, *4*). DA is the primary neurotransmitter released by DA neurons, and activation of DA receptors in postsynaptic neurons can modulate neuronal excitability and circuit output. It has recently been shown that GABA is copackaged with DA in midbrain DA neurons by the vesicular monoamine transporter 2 and is subsequently co-released in the striatum (*5*), where it provides direct and potent inhibition to postsynaptic striatal projection neurons through activation of GABA type A ($GABA_A$) receptors.

In the mammalian central nervous system (CNS), GABA biosynthesis is mediated by two glutamate decarboxylases (GAD65 and GAD67, 65- and 67-kD isoforms, respectively). Expression of either isoform of GAD has traditionally been used to identify GABAergic neurons in the CNS. To identify which subset of midbrain DA neurons is capable of GABA synthesis, we examined GAD expression in DA neurons by coupling immunohistochemistry for tyrosine hydroxylase (TH), the rate-limiting enzyme in DA synthesis, with in situ hybridization for *Gad1* or *Gad2* (which encode GAD67 and GAD65, respectively). Only a small percentage of midbrain DA neurons express *Gad* in the substantia nigra pars compacta (SNc, ~9%) (Fig. 1, A to K) and the ventral tegmental area (VTA, ~15%) (fig. S1) (*6*, *7*).

An individual DA neuron can extend elaborate axonal arbors covering large portions of the striatum (*8*). Consequently, even though GAD is expressed in only a small subset of DA neurons, it is possible that GAD-expressing neurons can drive sustained GABA co-release throughout the striatum. We thus asked whether GAD is required for GABAergic transmission in the striatum by recording alterations in dopaminergic inhibitory postsynaptic currents (IPSCs) in spiny projection neurons (SPNs) that resulted from pharmacological inhibition or conditional genetic deletion of GAD. The striatum comprises two parallel output pathways arising from distinct groups of "direct" and "indirect" pathway GABAergic SPNs (dSPNs and iSPNs, respectively) that differ in their expression of postsynaptic DA receptors coupled with heterotrimeric guanine nucleotide–binding protein. SPNs also send collateral inhibitory projections within the striatum. As SPNs express GAD and are considered conventional GABAergic neurons, we used striatal collateral inhibition as an internal control for our experiments. We expressed channelrhodopsin 2 (ChR2) in iSPNs by crossing A2A-Cre mice (in which Cre recombinase is selectively expressed in iSPNs but not in midbrain DA neurons) with transgenic mice containing a conditional floxed allele of ChR2 in the Rosa26 locus (Ai32 mice). Progeny from this cross were bred to Drd1a-tdTomato–expressing transgenic mice carrying a bacterial artificial chromosome transgene that selectively labels dSPNs. We then performed whole-cell voltage-clamp recordings in dSPNs in brain slices of dorsal striatum prepared from A2A-Cre;Ai32;Drd1a-tdTomato mice, in which ChR2 is selectively expressed in A2A adenosine receptor–expressing iSPNs and tdTomato expression is restricted to dopamine 1 (D1) receptor–expressing dSPNs. Optogenetic stimulation of iSPN axons with brief pulses (0.5 ms) of blue light (450 nm) reliably evoked IPSCs in dSPNs. Optogenetically evoked IPSCs (oIPSCs) recorded n dSPNs were isignificantly attenuated by GAD inhibitor 3-mercaptopropionic acid (3-MPA, 500 μM) (Fig. 1L), which confirmed that local collateral inhibitory transmission arising from iSPNs is dependent on GAD function. We next selectively deleted GAD in iSPNs (*9*), using *Gad1* and *Gad2* double conditional knockout mice (A2A-Cre;$Gad1^{fl/fl}$;$Gad2^{fl/fl}$). When recording oIPSCs from dSPNs in A2A-Cre;$Gad1^{fl/fl}$;$Gad2^{fl/fl}$;Ai32;Drd1a-tdTomato mice, we found that genetic deletion of both GADs in iSPNs abolished nearly all of the oIPSCs recorded in dSPNs. These data confirmed that GAD-mediated GABA synthesis is necessary for conventional GABAergic transmission within the striatum (Fig. 1L).

To test whether GAD is required for functional GABA co-release by midbrain DA neurons, whose axon terminals project onto SPNs, we used DAT-Cre;Ai32 mice to selectively express ChR2 in DA neurons (*5*, *10*) and recorded oIPSCs and oEPSCs in postsynaptic dorsal striatum SPNs. Monosynaptic oIPSCs and oEPSCs can be abolished by $GABA_A$ and glutamate-receptor blockers, respectively (fig. S2). To our surprise, neither incubating brain slices with 3-MPA (Fig. 1, M and N) nor genetically deleting both GAD isoforms in midbrain DA neurons using DAT-Cre;Ai32;$Gad1^{fl/fl}$;$Gad2^{fl/fl}$ mice (Fig. 1, O and P) significantly altered the amplitudes of oIPSCs and oEPSCs in SPNs, which indicated that midbrain DA neuron GABA co-released does not require canonical GAD-mediated GABA synthesis. GABA co-release from DA neurons was observed in recordings obtained throughout the striatum, in both dorsal and ventral regions. Notably, the oIPSCs recorded in dorsal striatum SPNs were significantly larger than those recorded from SPNs in the nucleus accumbens (NAc). Within NAc, oIPSC and oEPSC amplitudes were not significantly different between SPNs in the core or medial shell, and, as with oIPSCs recorded in dorsal striatum, oIPSCs recorded in the NAc were not blocked by application of 3-MPA (fig. S3). Recent work has suggested that DA can directly activate postsynaptic $GABA_A$ receptors (*11*). To exclude this possibility and test whether dopaminergic oIPSCs were caused by direct activation of $GABA_A$ receptors by DA, we locally applied DA and GABA onto individual SPNs and recorded IPSCs. Direct application of DA did not evoke IPSCs, whereas GABA successfully evoked IPSCs in the same SPN, which indicated that DA was not likely to be activating $GABA_A$ receptors directly in our cells. This idea was further supported by application of the DA transporter (DAT) blocker GBR12935, which elevates extracellular DA concentrations and similarly did not affect oIPSC amplitudes in the striatum (fig. S4). Together, these data suggest that dopaminergic oIPSCs were not caused by direct activation of $GABA_A$ receptors by DA.

[1]Department of Neurosurgery, Stanford University School of Medicine, Palo Alto, CA 94304, USA. [2]Department of Pathology, University of California San Francisco, San Francisco, CA 94143, USA. [3]Neuroscience Graduate Program, University of California San Francisco, San Francisco, CA 94143, USA. [4]Pathology Service 113B, San Francisco VA Medical Center, San Francisco, CA 94121, USA. [5]Department of Neurology and Neurological Sciences, Stanford University School of Medicine, Palo Alto, CA 94304, USA.
*Corresponding author. E-mail: dingjun@stanford.edu

In plants, GABA can be synthesized from putrescine (*12*) by the enzymes diamine oxidase (DAO) and aldehyde dehydrogenase (ALDH) (fig. S5A) (*13*, *14*). GABA production through this alternative evolutionarily conserved pathway also exists in *Xenopus* tadpole (*15*) and mammalian cells (*16*–*19*). Glial cells can also use putrescine to produce GABA during retinal early development (*18*, *20*). We tested whether ALDH-mediated alternative GABA synthesis drives GABA production in midbrain DA neurons. ALDH1a1 is the most abundant form of cytosolic ALDH (*21*, *22*) and is highly expressed in the ventral midbrain, including the region delineating the SNc (*23*) (for *Aldh1a1* mRNA) (*24*). We first examined ALDH expression in midbrain DA neurons by double immunostaining for ALDH1a1 and TH. ALDH1a1 is indeed highly expressed in a subset of DA neurons, colocalizing with TH in the SNc and VTA (Fig. 2, A to C, and fig. S5B). To examine subcellular localization of ALDH1a1, we injected an adeno-associated virus (AAV) carrying green fluorescent protein (GFP)–tagged ALDH1a1 into the midbrain and examined GFP expression in the striatum. We found that GFP strongly colocalizes with TH within axons in the dorsal striatum (Fig. 2D), which suggested that ALDH1a1 is highly abundant in dopaminergic terminals (fig. S5, C to F). We then tested the involvement of ALDH1a1 in GABA synthesis in these neurons by blocking its activity with the ALDH inhibitors 4-(diethylamino)-benzaldehyde (DEAB, 10 μM), or disulfiram (10 μM). To ensure that intracellular GABA levels were sufficiently depleted, we pretreated brain slices from DAT-Cre;Ai32 mice with artificial cerebrospinal fluid (ACSF) containing these blockers for 2 to 4 hours (a paradigm similar to our pharmacological treatment with 3-MPA targeting conventional GABA synthesis in SPNs). Treatment with both 4,4′-bis-(diethylamino)benzophenone (DEAB) and disulfiram dramatically reduced oIPSC amplitude in SPNs after DA axon stimulation (Fig. 2, E and F, and fig. S6, A and B). We also recorded oEPSCs in the same SPNs by stimulating DA fibers. Notably, this treatment did not affect the peak amplitude of oEPSCs (Fig. 2, E and F, and fig. S6, A and B), which suggested that these blockers do not prevent global neurotransmitter release, but rather selectively impair GABA co-release.

If GABA were indeed converted from putrescine, blocking DAO would also reduce GABA production. We thus used DAO blockers [aminoguanidine (AG), 100 μM, or amiloride, 10 μM] and examined the effect of each treatment on oIPSCs, using the same paradigm as above. Both AG and amiloride significantly and selectively reduced oIPSC amplitude in SPNs, with no effect on oEPSC amplitude (Fig. 2, G and H, and fig. S6, C and D) or on conventional GABAergic transmission (fig. S7). Notably, ALDH1a1 is known to be important for the synthesis of retinoic acid (RA) (*25*) and breakdown of the DA metabolite 3,4-dihydroxyphenylacetaldehyde to 3,4-dihydroxyphenylacetic acid (*26*). It is possible, then, that deletion of ALDH1a1 may lead to RA deficiency and a concomitant increase in extracellular DA concentration, both of which may have effects on synaptic transmission. Application of exogenous

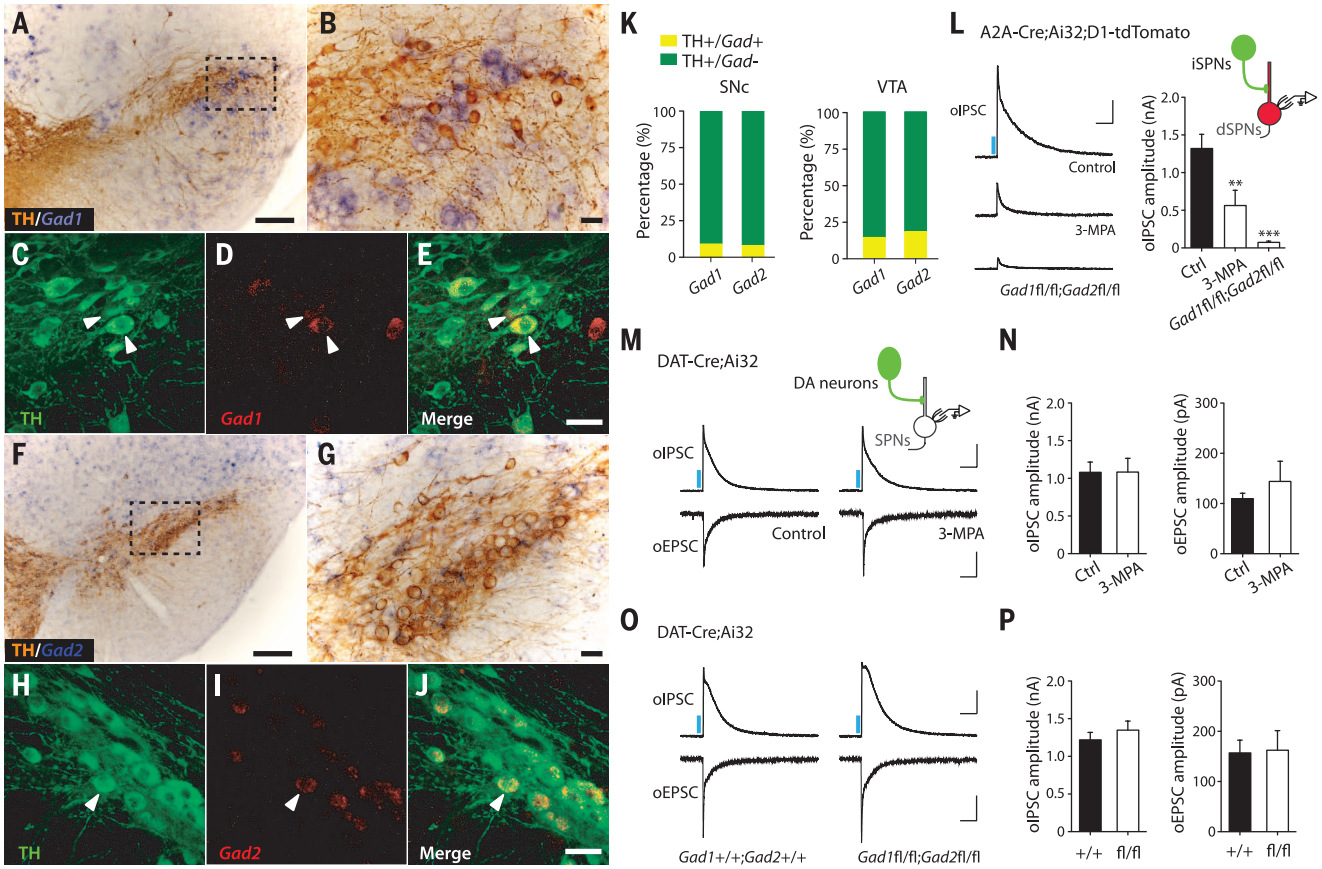

Fig. 1. GABA co-release by midbrain DA neurons does not require GAD. (**A** to **J**) Expression of *Gad1* and *Gad2* mRNA in DA neurons of the SNc. Immunolabeled TH-positive dopaminergic neurons (brown) combined with chromogenic in situ hybridization (ISH) for *Gad1* (A and B) and *Gad2* (F and G) mRNA. Confocal fluorescence images of ISH for *Gad1* (D) and *Gad2* (I) mRNA (red) combined with TH immunostaining (green) (C) to (E) and (H) to (J) show limited expression of *Gad* in TH$^+$ cells. (**K**) Quantification of TH/*Gad* colocalization in SNc (left) and VTA (right). (**L**) (Left) Representative oIPSC traces in control (top); 3-MPA–treated (500 μM) (middle); and *Gad1*$^{fl/fl}$;*Gad2*$^{fl/fl}$ (bottom) A2A-Cre;Ai32;Drd1a-tdTomato mice. (Right) Summary statistics for oIPSC recordings. Representative traces (**M**) and summary statistics (**N**) for oIPSC and oEPSC recorded from DAT-Cre;Ai32 mice treated with ACSF (control) and 3-MPA, respectively. Representative traces (**O**) and summary statistics (**P**) for oIPSC and oEPSC recorded from DAT-Cre;Ai32;*Gad1*$^{+/+}$;*Gad2*$^{+/+}$ and DAT-Cre;Ai32;*Gad1*$^{fl/fl}$;*Gad2*$^{fl/fl}$ mice. Blue bar indicates 450-nm light stimulation. Scale bars: 200 μm for (A) and (F), 50 μm for (B) to (E) and (G) to (J); current of 400 pA and time of 100 ms for oIPSC and 50 pA and 100 ms for oEPSC. Error bars indicate means ± SEM. $^{**}P < 0.01$, $^{***}P < 0.001$.

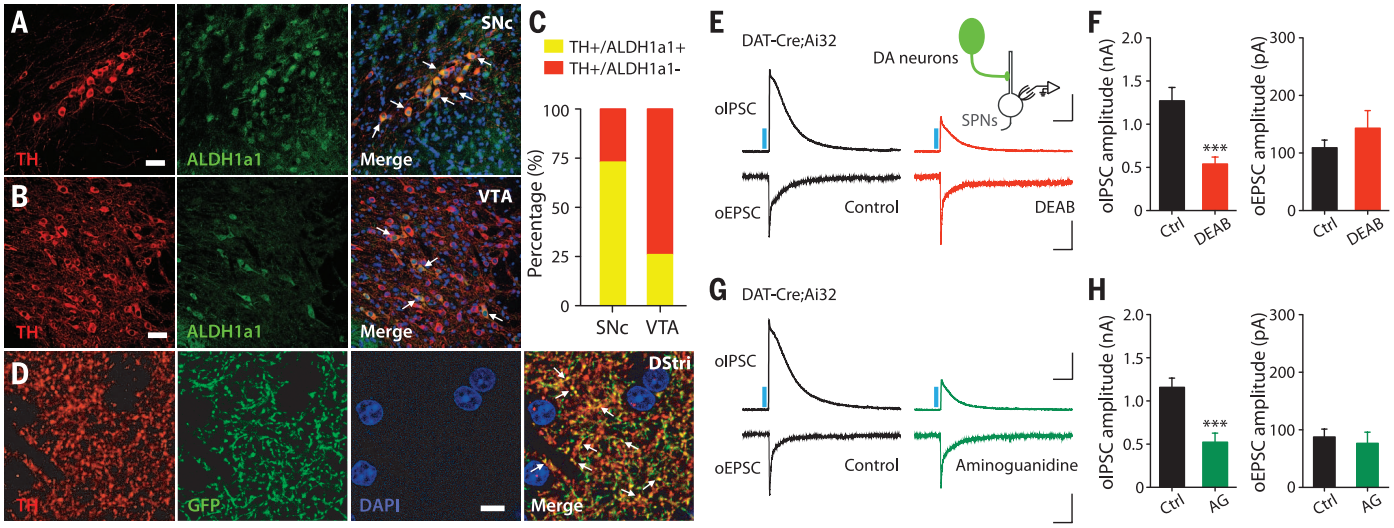

Fig. 2. ALDH1a1-mediated noncanonical GABA synthesis in DA neurons. (**A** and **B**) Confocal images depicting double immunostaining for TH (left, red) and ALDH1a1 (middle, green) in SNc (A) and VTA (B). Scale bar, 40 μm. (**C**) Quantification of ALDH1a1 expression in TH$^+$ DA neurons in SNc and VTA. (**D**) Confocal images depicting double immunostaining for TH (red), ALDH1a1-GFP (green), and 4′,6′-diamidino-2-phenylindole (DAPI) (blue) in the dorsal striatum (DStri). Scale bar, 10 μm. Representative oIPSC and oEPSC traces (**E**) and summary statistics (**F**) recorded from DAT-Cre;Ai32 mice treated with ACSF (control, left) and DEAB (10 μM, right). Representative oIPSC and oEPSC traces (**G**) and summary statistics (**H**) recorded from DAT-Cre;Ai32 mice treated with ACSF (control, left) and AG (100 μM, right). Blue bar indicates 450-nm light stimulation. Scale bars: 400 pA and 100 ms for oIPSC and 50 pA and 100 ms for oEPSC. Error bars indicate means ± SEM. ***$P < 0.001$. The arrows in (A), (B), and (D) highlight the colocalization of TH and ALDH1a1.

Fig. 3. *Aldh1a1* knockdown and genetic deletion reduce dopaminergic oIPSCs and are rescued by *Aldh1a1* overexpression. (**A**) Schematic illustration depicting viral shRNA constructs (*Aldh1a1** indicates an shRNA-resistant WT *Aldh1a1*) and experimental configuration. Stri, striatum. (**B**) Confocal image showing expression of shRNA (green) in TH$^+$ (red) neurons. Arrowheads indicate absence of ALDH1a1 (blue) in GFP$^+$/TH$^+$ neurons. Scale bar, 20 μm. Representative oIPSC and oEPSC traces (**C**) and summary statistics (**D**) in DAT-Cre;Ai32 mice injected with *Aldh1a1* knockdown and rescue viruses. Representative oIPSC and oEPSC traces (**E**) and summary statistics for oIPSC (**F**) and oEPSC (**G**) in *Aldh1a1*$^{+/+}$;DAT-Cre;Ai32 or *Aldh1a1*$^{-/-}$;DAT-Cre;Ai32 mice, or loss-of-function mice treated with DEAB (10 μM) or AG (100 μM). Representative oIPSC and oEPSC traces (**H**) and summary statistics (**I**) recorded from *Aldh1a1*$^{-/-}$;DAT-Cre;Ai32 mice injected with control and rescue viruses. Blue bar indicates 450-nm light stimulation. Scale bars: 400 pA and 100 ms for oIPSC and 50 pA and 100 ms for oEPSC. Error bars indicate means ± SEM. *$P < 0.05$, **$P < 0.01$, ***$P < 0.001$.

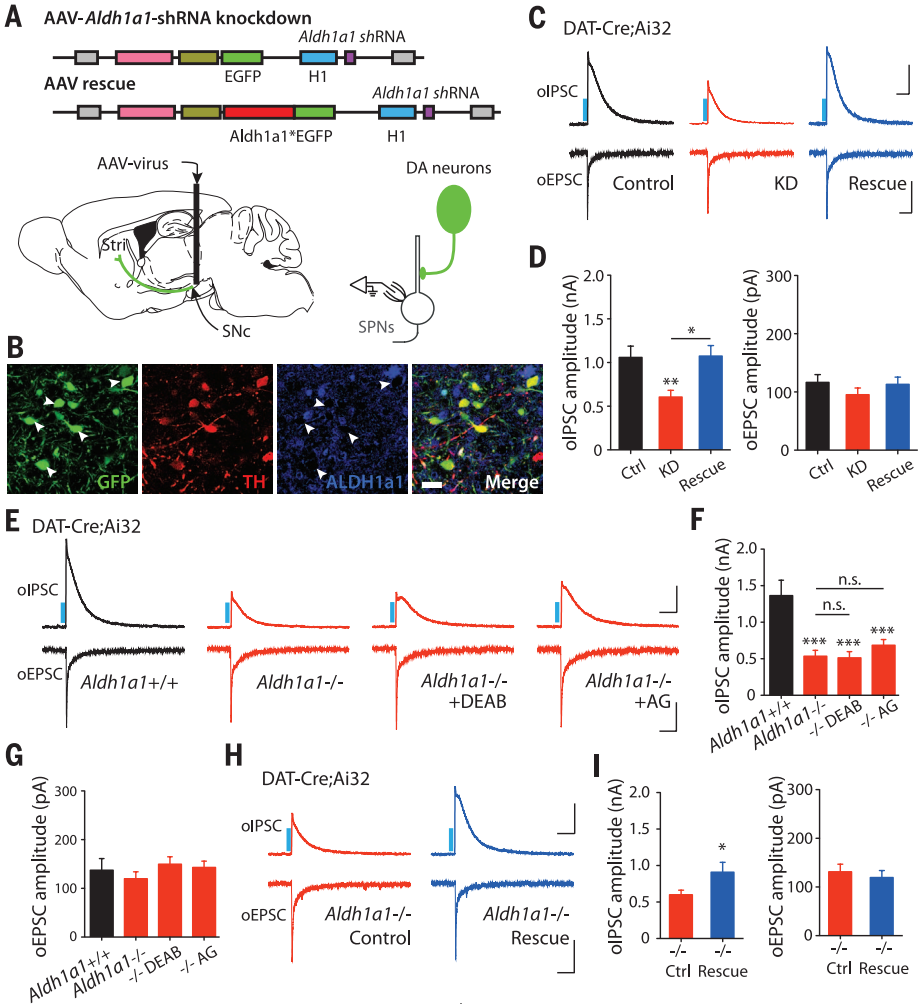

RA and a D2 receptor antagonist (sulpiride), however, did not prevent observed reduction of oIPSCs in SPNs and had no effect on oEPSCs, which suggested that these other ALDH1a1-mediated functions are not important for GABA co-release (fig. S8).

To selectively manipulate ALDH1a1 expression in midbrain DA neurons, we injected an AAV-expressing short hairpin RNA (shRNA) targeted against *Aldh1a1* into the ventral midbrain of DAT-Cre;Ai32 mice to reduce the supply of the gene or [knockdown (KD)] and so reduce *Aldh1a1* expression (Fig. 3, A and B, and fig. S9). *Aldh1a1* KD in the midbrain significantly reduced oIPSC amplitude in SPNs (Fig. 3, C and D), an effect that was fully rescued by simultaneous expression of an shRNA-resistant wild-type (WT) *Aldh1a1* (Aldh1a1*) (Fig. 3, C and D). Notably, *Aldh1a1* KD and rescue had no effect on oEPSCs recorded in the same neurons. These data suggest that presynaptic expression of ALDH1a1 in DA neurons is critical for GABA synthesis and co-release.

We next asked whether genetic deletion of ALDH1a1 can selectively diminish GABA corelease by midbrain DA neurons (*27*). We recorded oIPSCs and oEPSCs in SPNs from the dorsal striatum of *Aldh1a1*$^{-/-}$;DAT-Cre;Ai32 transgenic mice and *Aldh1a1*$^{+/+}$ littermate controls. Dopaminergic oIPSCs were strongly attenuated in *Aldh1a1*$^{-/-}$ mice, whereas oEPSCs were unaffected (Fig. 3, E to G). Because ALDH1a1 is the final enzyme in the conversion process leading to GABA synthesis, the pharmacological effects of DAO and ALDH blockers should be occluded by *Aldh1a1* deletion. We treated brain slices from *Aldh1a1*$^{-/-}$; DAT-Cre;Ai32 with DAO and ALDH blockers and found that DAO and ALDH blockers did not further reduce oIPSC amplitude in SPNs in *Aldh1a1*$^{-/-}$ mice (Fig. 3, E to G). As an additional control, we examined oIPSCs in *Aldh1a1*$^{-/-}$;A2A-Cre;Ai32;Drd1a-tdTomato mice resulting from collateral intrastriatal inhibition and confirmed that conventional GABA transmission is not affected in mutant mice (fig. S10). Last, we tested whether elevated expression of *Aldh1a1* could rescue the reduction of dopaminergic IPSCs observed in SPNs in *Aldh1a1*$^{-/-}$ mice. To achieve this, we injected AAV-rescue constructs into the midbrain of *Aldh1a1*$^{-/-}$;DAT-Cre;Ai32 mice and subsequently recorded oIPSCs in SPNs. Overexpression of *Aldh1a1* fully rescued the dopaminergic oIPSCs in SPNs without affecting oEPSCs (Fig. 3, H and I). GABA transporters also contribute to the accumulation of presynaptic GABA in midbrain DA neurons (fig. S11). Taken together, our data suggest that ALDH1a1-mediated alternative GABA synthesis supports functional GABAergic transmission by DA neurons.

Mutations of *aldh1a1* have been linked to alcoholism in human populations (*28*, *29*), which suggests that GABA co-release by DA neurons may be altered by drug abuse. Given the involvement of the dopaminergic system and dorsal striatum in enhanced alcohol consumption, preference, and addiction (*30*–*32*), we examined GABA co-release in mice exposed to repeated in vivo administration and withdrawal of EtOH, a behavioral paradigm approximating binge drinking episodes in humans. Intoxicating levels of EtOH were administered (2 g/kg ETOH, 20%, intraperitoneal injection) daily for seven consecutive days (*32*). Two to 4 hours after the final EtOH injection, we prepared striatal brain slices from DAT-Cre;Ai32 mice and recorded oIPSCs in SPNs. We found that repeated in vivo administration of EtOH significantly decreased oIPSC, but not oEPSC, amplitude recorded in SPNs (Fig. 4, A and B). We then tested whether a direct EtOH treatment can affect GABA co-release in brain slices. To mimic blood alcohol levels after binge drinking, we pretreated striatal brain slices for 2 to 4 hours (paradigm comparable to our previous pharmacological manipulations) with EtOH at concentrations comparable to blood alcohol levels during binge-drinking episodes (17 to 50 mM). Prolonged, but not acute, treatment with 17 to 50 mM EtOH significantly decreased the oIPSCs amplitude recorded in SPNs after DA axon stimulation (Fig. 4, C and D). The same EtOH treatments did not affect oEPSC amplitude or that of oIPSCs recorded from dSPNs in A2A-Cre;Ai32;Drd1a-tdTomato mice (fig. S12). Reduction of GABA co-release was not observed in *Aldh1a1*$^{-/-}$ mice (fig. S13), which suggested that EtOH modulation is dependent on ALDH1a1. Our results indicate that GABA co-release is attenuated by EtOH at blood alcohol concentrations similar to those measured after binge drinking. As excessive alcohol drinking enhances the inclination for alcohol drinking behavior (*33*), we used the home cage continuous two-bottle-choice test to evaluate behavioral consequences of ALDH1a1 deletion on EtOH intake (*34*). Basal locomotion, as assessed by an open-field test, remains intact in

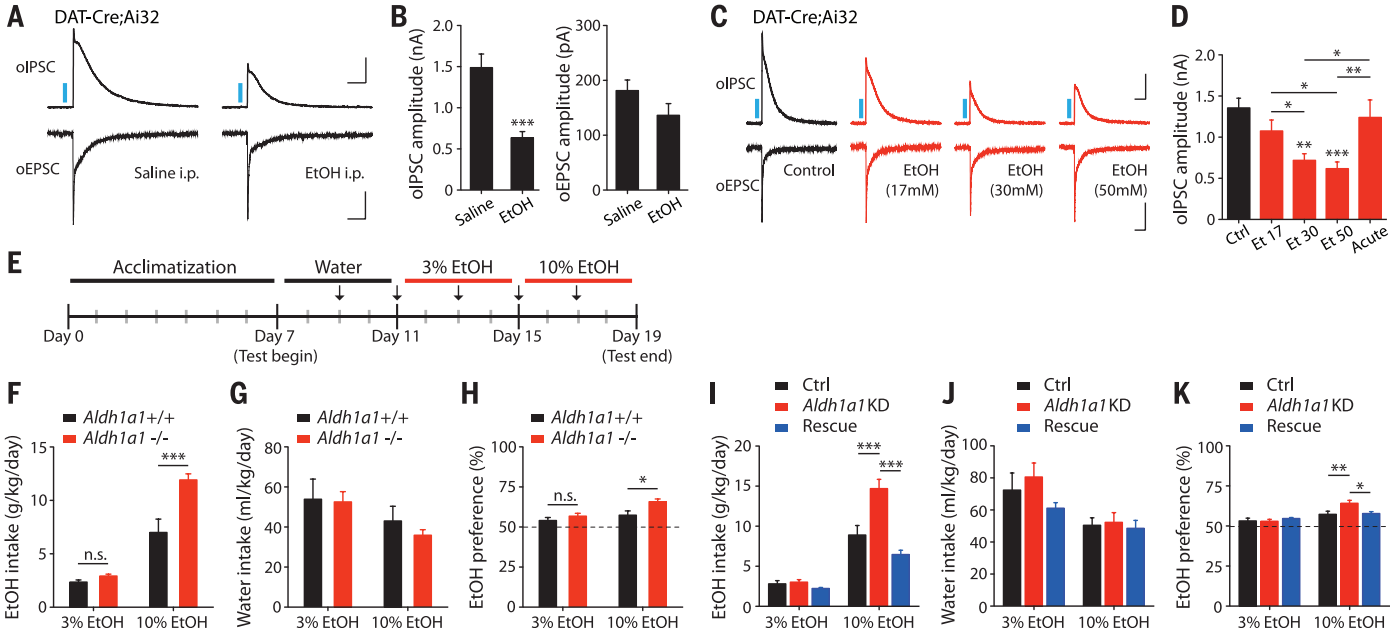

Fig. 4. Altered GABA co-release in conditions related to alcohol binge drinking. Representative oIPSC and oEPSC traces (**A**) and summary statistics (**B**) in DAT-Cre;Ai32 mice in control or after repeated in vivo administration of EtOH. Representative oIPSC and oEPSC traces (**C**) and summary statistics (**D**) in DAT-Cre;Ai32 mice in control mice or mice treated with EtOH (17 to 50 mM). (**E**) Shematic illustration depicting the timeline of the two-bottle-choice behavioral assay. (**F**) Quantification of average daily EtOH intake, (**G**) average daily water intake, and (**H**) average EtOH preference. (**I**) Quantification of average daily EtOH intake in *Aldh1a1* KD or *Aldh1a1* overexpression mice. (**J**) Average daily water intake. (**K**) Average EtOH preference. Blue bar indicates 450-nm light stimulation. Scale bars: 400 pA and 100 ms for oIPSC and 50 pA and 100 ms for oEPSC. Error bars indicate means ± SEM. *$P < 0.05$, **$P < 0.01$, ***$P < 0.001$.

Aldh1a1$^{-/-}$ mice (fig. S14). When given continuous access to EtOH, *Aldh1a1*$^{-/-}$ mice significantly increased their intake of and preference for EtOH, with no significant difference in daily water intake, compared with WT littermates (Fig. 4, E to H). To more conclusively demonstrate that loss of ALDH1a1 specifically in midbrain neurons is responsible for enhanced EtOH consumption, we injected an AAV-expressing *Aldh1a1*-shRNA into the ventral midbrain of WT mice to knockdown *Aldh1a1* expression (fig. S9). *Aldh1a1* KD in the midbrain recapitulated the behavioral phenotype in which increased intake of and preference for EtOH is observed in *Aldh1a1*$^{-/-}$ mice. This behavioral effect was fully rescued by simultaneous expression of an shRNA-resistant WT *Aldh1a1** (Fig. 4, I to K). Together, our studies suggest that diminished GABA co-release may serve as a potential determinant for enhanced alcohol consumption and preference.

Midbrain DA neurons are known to act through slow neuromodulatory mechanisms. However, GABA co-release in DA neurons demonstrates a rapid and potent inhibitory control used by DA neurons. A variety of neuronal subtypes can co-release multiple neurotransmitters in different neural circuits (*35*–*37*). How an individual neuron releases and regulates multiple neurotransmitters remains unclear. We found that DA neurons use an alternative GABA synthesis pathway to support functional GABAergic neurotransmission. Co-released GABA can permit very local inhibition of dendritic excitability, a key mechanism controlling synaptic plasticity. Moreover, as this pathway is evolutionarily conserved and given the widespread expression of ALDH1 in a variety of cell types—including cells of the retina (*19*, *20*) and hippocampus (*21*), and a subset of SPNs (fig. S5), our findings suggest that GABA alternative synthesis may represent a more fundamental mechanism used by broader classes of GABAergic neurons.

The dorsal striatum plays important roles in the transitioning from initial voluntary drug use to habitual, and ultimately compulsive, drug abuse (*30*, *38*, *39*). The GABAergic synapse has also been the focus of extensive study for its role in the behavioral consequences of EtOH exposure. In particular, it has been suggested that acute and chronic EtOH exposure modulate GABAergic release and synaptic $GABA_A$ receptors through pre- and postsynaptic mechanisms, respectively (*40*). Our studies indicate that EtOH attenuates GABA co-release by inhibiting GABA biosynthesis at concentrations similar to those after binge-drinking alcohol, which provides an additional mechanism through which EtOH exposure can modulate the activity of GABAergic synapses. Diminished GABA co-release and ALDH1a1 activity may directly contribute to enhancement of alcohol intake and preference behavior, reminiscent of humans with *Aldh1a1* mutations. In evaluating genetic factors associated with risk of alcohol abuse then, we will likely need to consider pre- and postsynaptic components that converge on the GABAergic system. Together, our data indicate that GABA co-release, in addition to DA, may serve an essential function in the regulation of the development of addictive behaviors.

REFERENCES AND NOTES

1. W. Schultz, *Annu. Rev. Neurosci.* **30**, 259–288 (2007).
2. N. X. Tritsch, B. L. Sabatini, *Neuron* **76**, 33–50 (2012).
3. B. T. Chen, F. W. Hopf, A. Bonci, *Ann. N. Y. Acad. Sci.* **1187**, 129–139 (2010).
4. P. Redgrave *et al*., *Nat. Rev. Neurosci.* **11**, 760–772 (2010).
5. N. X. Tritsch, J. B. Ding, B. L. Sabatini, *Nature* **490**, 262–266 (2012).
6. T. González-Hernández, P. Barroso-Chinea, A. Acevedo, E. Salido, M. Rodríguez, *Eur. J. Neurosci.* **13**, 57–67 (2001).
7. N. X. Tritsch, W. J. Oh, C. Gu, B. L. Sabatini, *eLife* **3**, e01936 (2014).
8. W. Matsuda *et al*., *J. Neurosci.* **29**, 444–453 (2009).
9. C. L. Heusner, L. R. Beutler, C. R. Houser, R. D. Palmiter, *Genesis* **46**, 357–367 (2008).
10. S. Lammel *et al*., *Neuron* **85**, 429–438 (2015).
11. P. Hoerbelt, T. A. Lindsley, M. W. Fleck, *J. Neurosci.* **35**, 3525–3536 (2015).
12. K. Williams, *Cell. Signal.* **9**, 1–13 (1997).
13. S. G. Xing, Y. B. Jun, Z. W. Hau, L. Y. Liang, *Plant Physiol. Biochem.* **45**, 560–566 (2007).
14. B. J. Shelp *et al*., *Plant Sci.* **193-194**, 130–135 (2012).
15. M. R. Bell, J. A. Belarde, H. F. Johnson, C. D. Aizenman, *Nat. Neurosci.* **14**, 505–512 (2011).
16. E. B. Sequerra, P. Gardino, C. Hedin-Pereira, F. G. de Mello, *Neuroscience* **146**, 489–493 (2007).
17. T. Noto *et al*., *Pharmacol. Biochem. Behav.* **25**, 411–414 (1986).
18. E. N. Yamasaki, V. D. Barbosa, F. G. De Mello, J. N. Hokoc, *Int. J. Dev. Neurosci.* **17**, 201–213 (1999).
19. J. Laschet, T. Grisar, M. Bureau, D. Guillaume, *Neuroscience* **48**, 151–157 (1992).
20. B. A. Barres, W. J. Koroshetz, K. J. Swartz, L. L. Chun, D. P. Corey, *Neuron* **4**, 507–524 (1990).
21. J. Aoto, C. I. Nam, M. M. Poon, P. Ting, L. Chen, *Neuron* **60**, 308–320 (2008).
22. G. Liu *et al*., *J. Clin. Invest.* **124**, 3032–3046 (2014).
23. P. McCaffery, U. C. Dräger, *Proc. Natl. Acad. Sci. U.S.A.* **91**, 7772–7776 (1994).
24. Allen Brain Atlas, http://mouse.brain-map.org/gene/show/11455.
25. V. Vasiliou, A. Pappa, D. R. Petersen, *Chem. Biol. Interact.* **129**, 1–19 (2000).
26. D. S. Goldstein *et al*., *J. Neurochem.* **126**, 591–603 (2013).
27. X. Fan *et al*., *Mol. Cell. Biol.* **23**, 4637–4648 (2003).
28. R. Sherva *et al*., *Alcohol. Clin. Exp. Res.* **33**, 848–857 (2009).
29. J. Liu *et al*., *Alcohol. Clin. Exp. Res.* **35**, 304–316 (2011).
30. B. J. Everitt, T. W. Robbins, *Nat. Neurosci.* **8**, 1481–1489 (2005).
31. G. Chen *et al*., *Alcohol. Clin. Exp. Res.* **35**, 1739–1748 (2011).
32. J. Wang *et al*., *J. Neurosci.* **32**, 15124–15132 (2012).
33. L. E. O'Dell, A. J. Roberts, R. T. Smith, G. F. Koob, *Alcohol. Clin. Exp. Res.* **28**, 1676–1682 (2004).
34. S. Ben Hamida *et al*., *J. Neurosci.* **33**, 14369–14378 (2013).
35. T. S. Hnasko *et al*., *Neuron* **65**, 643–656 (2010).
36. D. H. Root *et al*., *Nat. Neurosci.* **17**, 1543–1551 (2014).
37. S. J. Shabel, C. D. Proulx, J. Piriz, R. Malinow, *Science* **345**, 1494–1498 (2014).
38. D. M. Lovinger, *Neuropharmacology* **58**, 951–961 (2010).
39. C. M. Pennartz *et al*., *J. Neurosci.* **29**, 12831–12838 (2009).
40. J. L. Weiner, C. F. Valenzuela, *Pharmacol. Ther.* **111**, 533–554 (2006).

ACKNOWLEDGMENTS

The authors thank A. Du and Y. Liu for technical assistance; D. Ron for suggestions on using the two-bottle-choice behavior test; and T. Sudhof, G. Panagiotakos, W. Wei, Z. Khaliq, and members of the Ding laboratory for helpful discussions. Supported by grants from the National Institute of Neurological Disorders and Stroke, NIH, NS075136, NS091144 (J.B.D.), the Klingenstein Foundation (J.B.D.), and National Institute of Mental Health, NIH, MH086403 (L.C.) and MH091193 (L.C.). The authors declare no conflicts of interest. All primary electrophysiological and immunohistochemical data are archived on a server in the Department of Neurosurgery at Stanford University School of Medicine.

SUPPLEMENTARY MATERIALS

www.sciencemag.org/content/350/6256/102/suppl/DC1
Materials and Methods
Figs. S1 to S14
Table S1
References (*41*–*51*)

29 April 2015; accepted 25 August 2015
10.1126/science.aac4690

STRUCTURAL BIOLOGY

Crystal structure of the metazoan Nup62•Nup58•Nup54 nucleoporin complex

Hema Chug, Sergei Trakhanov, Bastian B. Hülsmann, Tino Pleiner, Dirk Görlich*

Nuclear pore complexes (NPCs) conduct nucleocytoplasmic transport and gain transport selectivity through nucleoporin FG domains. Here, we report a structural analysis of the FG Nup62•58•54 complex, which is a crucial component of the transport system. It comprises a ≈13 nanometer-long trimerization interface with an unusual 2W3F coil, a canonical heterotrimeric coiled coil, and a kink that enforces a compact six-helix bundle. Nup54 also contains a ferredoxin-like domain. We further identified a heterotrimeric Nup93-binding module for NPC anchorage. The quaternary structure alternations in the Nup62 complex, which were previously proposed to trigger a general gating of the NPC, are incompatible with the trimer structure. We suggest that the highly elongated Nup62 complex projects barrier-forming FG repeats far into the central NPC channel, supporting a barrier that guards the entire cross section.

Nuclear pore complexes (NPCs) are embedded into the nuclear envelope and built from nucleoporins (Nups). They conduct nucleocytoplasmic transport in order to supply the cell nucleus with proteins and the cytoplasm with ribosomes, mRNA, and tRNAs. The NPC framework is of eightfold rotational symmetry and assembled from the Nup155•Nup35•Nup93•Nup188/205 complex, as well as the

Department of Cellular Logistics, Max Planck Institute for Biophysical Chemistry, Göttingen, Germany.
***Corresponding author. E-mail: goerlich@mpibpc.mpg.de**

Science
AAAS

Aldehyde dehydrogenase 1a1 mediates a GABA synthesis pathway in midbrain dopaminergic neurons

Jae-Ick Kim *et al.*

Science **350**, 102 (2015);
DOI: 10.1126/science.aac4690

Science (print ISSN 0036-8075; online ISSN 1095-9203) is published weekly, except the last week in December, by the American Association for the Advancement of Science, 1200 New York Avenue NW, Washington, DC 20005.